

Phyllotaxis of Flux Lattices in Layered Superconductors

L. S. Levitov^(a)

L. D. Landau Institute for Theoretical Physics, Kosygin st. 2, 117940, Moscow, GSP-1, U.S.S.R.

(Received 24 August 1990)

The geometry of a flux lattice pinned by superconducting layers is studied. Under variation of magnetic field the lattice undergoes an infinite sequence of continuous transitions corresponding to different ways of selection of shortest distances. All possible lattices form a hierarchical structure identified as the hierarchy of Farey numbers. It is shown that dynamically accessible lattices are characterized by pairs of consecutive Fibonacci numbers.

PACS numbers: 74.60.Ge, 74.70.Jm

The phenomenon of phyllotaxis is a morphological property of many botanical objects: leaves of various plants, seeds of a pinecone and of a sunflower, scales of a pineapple, etc.^{1,2} They are arranged in lattices formed by spirals, left hand and right hand, whose numbers are always found to be consecutive in the Fibonacci sequence. Recently an interesting mechanism of phyllotaxis was suggested: compression-induced evolution of hard disks packed along logarithmic spirals.² In this Letter we study a physical system lying far away from botanics: an Abrikosov flux lattice in a layered superconductor. Surprisingly, it turns out that the dynamics of the lattice under variation of magnetic field gives rise to structures very similar to those known in botanics. In particular, pairs of consecutive Fibonacci numbers appear. Besides opening a way to an alternative explanation of botanical phyllotaxis,³ this result suggests that phyllotaxis is a general phenomenon that must occur in all soft lattices subjected to strong deformation.

Let us describe precisely the situation we are interested in. We consider a layered superconductor having zero-temperature correlation length ξ_0 comparable to the interlayer spacing d . In this case at sufficiently low temperature $T < T_c$ the layered structure provides strong pinning of superconducting vortices.^{4,5} To simplify the discussion we assume that both the magnetic field H and the vortices are parallel to the superconducting layers.⁶ Our gedanken experiment will consist of two steps: (1) lowering the temperature T while keeping H constant; (2) then lowering the magnetic field H at $T = \text{const}$.

So, we start with $T > T_c$ and $H_{c1} < H < H_{c2}$, where H_{c1} and H_{c2} are the zero-temperature critical fields. First, when we lower the temperature, superconductivity emerges at $T = T_c(H)$ and vortices appear. The optimal vortex lattice appearing at $T_c(H)$ is triangular and symmetric, the families of its symmetry planes being parallel and perpendicular to the planes of the layers.⁷ Near $T_c(H)$, pinning by the layers is weak because of thermal fluctuations, but it becomes stronger as we keep going down in temperature. For what will be done below it is important to assume that the temperature T we have reached is small enough to provide locking of the vortices between the layers for the whole time of our experiment. Now, when we start varying H in this low-temperature state the vortices are free to move only in the planes

separating the layers and, because of this, a shear instability develops at some critical H_0 .⁸ Moreover, below H_0 the lattice undergoes an infinite sequence of transitions generating Fibonacci numbers.

Let us specify the configurations of vortices we are considering and write the Hamiltonian. Everywhere below we study only vortices arranged in a periodic lattice. Roughly speaking, our reason for this is the following: The vortices interact repulsively at all distances and a general belief exists (although not proven yet) that only simple periodic structures are favored by repulsive interactions.⁹ Because of the symmetry mentioned above the starting lattice consists of periodic arrays of vortices aligned along the planes of the layers (indicated by horizontal rows in the inset of Fig. 1), vortices in neighboring rows being shifted by $a/2$. Since the vortices can move only along the planes, the class of lattices we have to analyze is a two-parameter family: $a > 0$, $0 < a < 1$ (due to pinning $b = \text{const}$). It is worth remarking here that the value of b is set by the starting magnetic field, so the horizontal rows of vortices are likely to be separated by many layers: $b \gg d$. Whenever the configuration of vortices is given its energy can be obtained from the theory of superconductivity. Because of the condition $b \gg d$ a simple expression derived from anisotropic Lon-

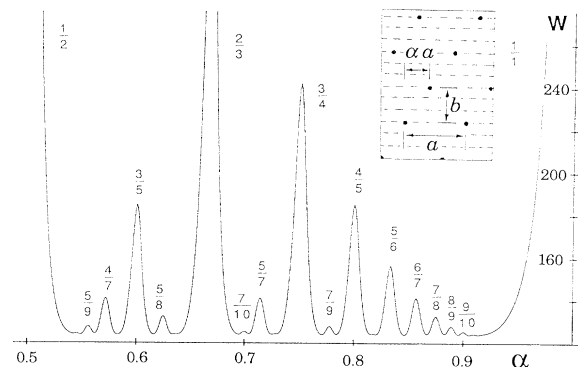


FIG. 1. The function $W_x(a)$ for $0.5 < a < 1$, $x = 0.015$. The peaks are marked by rational numbers corresponding to zeros of $\sin(\pi a n)$ in (2). Inset: Flux lattice. Planes of superconducting layers are indicated by dashed lines. Because of pinning b is never changed. The starting (symmetric) lattice corresponds to $a = \frac{1}{2}$.

don equations¹⁰ can be used:

$$F = Z \sum_{mn} [1 + \lambda^2 (\mu_1 G_x^2 + \mu_3 G_y^2)]^{-1}, \quad (1)$$

$$G_x = 2\pi n/a, \quad G_y = 2\pi(m - an)/b,$$

where $Z = \Phi_0^2/a^2 b^2 8\pi$, λ is London penetration depth, and μ_1, μ_3 are eigenvalues of the mass tensor.⁷ The sum (1) runs over the reciprocal lattice $\mathbf{G}_{mn} = (G_x, G_y)$, where m and n are integers. As a result of quantization of flux we have a relation between the magnetic field H and the area of the unit cell: $\Phi_0 = abH$. Therefore, whenever H is chosen, a is fixed. Thus our task becomes straightforward: For any given H (or a) study minima of the energy F as function of α . This will be carried out below in the two limiting cases: (i) $a, b \ll \lambda$ and (ii) $a, b \gg \lambda$. The first case is very easy to analyze numerically, while the second allows for analytic solution. The results in the cases (i) and (ii) turn to be qualitatively and even quantitatively similar.

In the first case the repulsion of the vortices is logarithmic, i.e., one can neglect the 1 in the denominator of (1) and, after summing over m , obtain

$$W_x(\alpha) = -Z_1 \sum_{n>0} \frac{\sin^2(\pi n \alpha)}{\sinh^2(n x) + \sin^2(\pi n \alpha)} \frac{\coth(n x)}{n x}, \quad (2)$$

where $x = a_0/a$, $a_0 = \pi b (\mu_1/\mu_3)^{1/2}$, and $Z_1 = Z b^2/4\mu_3$. After combining this with $\Phi_0 = abH$ we get the relation $x = cH$, where $c = a_0 b/\Phi_0$. So, x turns out to be the dimensionless magnetic field of the problem. Let us remark that when (2) was obtained from (1) an irrelevant constant was added to cancel a large but α -independent part of F .

The function $W_x(\alpha)$ has simple symmetry properties: $W_x(\alpha) = W_x(\alpha+1) = W_x(-\alpha)$. Because of that we study it only in the interval $0.5 < \alpha < 1$. Qualitatively, the behavior of $W_x(\alpha)$ can be understood in the following way. The denominator $\sinh^2(n x) + \sin^2(\pi n \alpha)$ of the n th term of (2) produces a peak near every rational $\alpha_{mn} = m/n$ provided $n \leq x^{-1}$; otherwise, the peak is smoothed out. So, for any given $x \ll 1$ the plot $W_x(\alpha)$ exhibits peaks near all rationals α_{mn} with denominators less than x^{-1} (see Fig. 1). Thus at small x the function $W_x(\alpha)$ has approximately x^{-2} local maxima and about the same number of local minima, since maxima and minima alternate. An interesting feature of the minima clearly seen in Fig. 1 is that they all have roughly equal energy. Because of that we are forced to study all the minima together.

The positions of all minima plotted as functions of x give the picture shown in Fig. 2. The first thing to note is that at high x there is a single minimum located at $\alpha = 0.5$ corresponding to the stability of the symmetric lattice. Then, when going down in x , a bifurcation occurs at $x \approx 0.24$ (the shear instability of the lattice leads to symmetry breaking⁸). Another point is that at small x many new minima appear, forming a complex

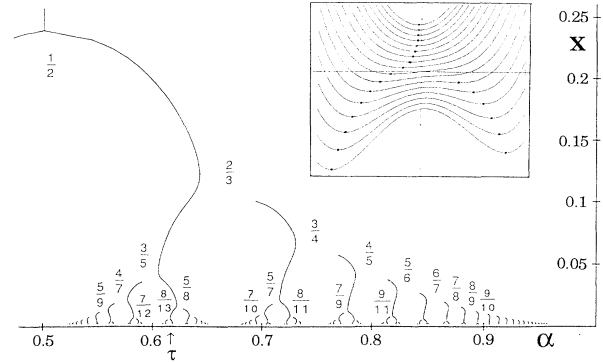


FIG. 2. Positions of local minima of the function $W_x(\alpha)$ as functions of x . Quasibifurcations are labeled by rational numbers corresponding to the peaks of $W_x(\alpha)$. The trajectory of the minimum starting at the bifurcation point $\alpha = \frac{1}{2}$ passes through quasibifurcations labeled by $\frac{1}{2}, \frac{2}{3}, \frac{3}{5}, \frac{5}{8}, \frac{8}{13}$, fractions composed of consecutive Fibonacci numbers. Its limit τ , the golden mean, is marked. Inset: A quasibifurcation occurring in asymmetric potential.

hierarchical structure. However, only two of them are dynamically accessible from the bifurcation point. We shall see below that as $x \rightarrow 0$ the two accessible minima tend to τ and $1 - \tau$, where $\tau = (\sqrt{5} - 1)/2 \approx 0.618$ is the golden mean. It is worth mentioning that the geometry of Fig. 2 is remarkably similar to the branching pattern found by Koch and Rothen.²

To get a further understanding of Fig. 2 we observe that although only one true bifurcation of minima occurs, the whole pattern can be viewed as resulting from “quasibifurcations.” The mechanism of a quasibifurcation is shown in the inset of Fig. 2. Every quasibifurcation can be attributed to the appearance of a new peak of the function $W_x(\alpha)$. As we have seen, the peaks can be labeled by rational numbers. Now we are able to transport this labeling to Fig. 2. The rational labels put on Fig. 2 help to reveal an interesting number-theoretic structure underlying the pattern. It turns to be nothing but the hierarchy of Farey numbers.

Farey numbers¹¹ are just all rational numbers between 0 and 1 arranged in series \mathcal{F}_n , each consisting of 2^n numbers (see Fig. 3). A simple rule allows one to compute \mathcal{F}_{n+1} provided all previous series are known: Order the numbers of the first n series, then put between every two neighbors their “sum” according to the Farey rule $p/q \oplus r/s = (p+r)/(q+s)$. (To be able to apply this rule to \mathcal{F}_1 it is convenient to introduce $\mathcal{F}_{-1} = \{0/1, 1/1\}$ as shown in Fig. 3.) This generation rule implies that every two numbers of \mathcal{F}_n are separated by at least one number from \mathcal{F}_{n-1} . In turn, this means that every number appears in Farey series as a sum of two numbers belonging to *different* series. Thus every number has a “younger” and an “older” parent. Let us connect every number with its younger parent (as shown in Fig. 3). Remarkably, we can observe that the structure we get has the same branching properties as the one in Fig. 2.

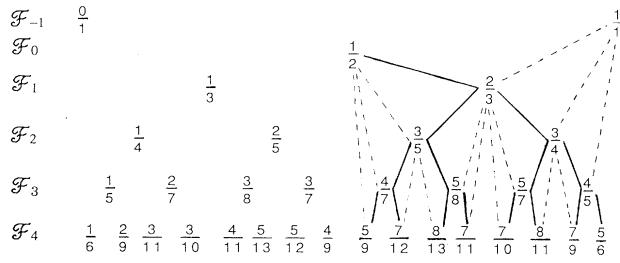


FIG. 3. Farey numbers arranged in series \mathcal{F}_n . Each number m/n is connected with its "parents" p/q and r/s in preceding series ($m=p+r, n=q+s$). Connections with younger (older) parents are shown by solid (dashed) bonds.

Now we want to extrapolate the Farey law found empirically in the computed part of the pattern (Fig. 2) to *all* arbitrarily small x . An important consequence of this extrapolation is that the trajectory of the dynamically accessible minimum (starting at $\alpha=0.5$) goes through the sequence of quasibifurcation points labeled by the fractions F_n/F_{n+1} , where F_n are Fibonacci numbers. [Proof: (i) Fibonacci numbers satisfy $F_{n+1} = F_n + F_{n-1}$; (ii) every three subsequent numbers $n_1/m_1, n_2/m_2, n_3/m_3$ on the continuous curves in Fig. 3 formed by solid lines satisfy the Farey rule $n_3 = n_2 + n_1, m_3 = m_2 + m_1$.] We also immediately get that the limit of the dynamically accessible minimum is the golden mean since this is the property of the ratios of Fibonacci numbers. Let us also mention another interesting feature of Fig. 2 following from this analysis: The set of limiting points of all trajectories fills densely the interval $[0.5, 1]$ (because the Farey numbers of the series \mathcal{F}_n become dense in $[0, 1]$ as $n \rightarrow \infty$).

Now let us switch to the case $a, b \gg \lambda$ corresponding to exponentially weak repulsion of the vortices. Certainly, this situation is of less experimental interest than the one of logarithmic repulsion discussed above: When the repulsion is small the lattice becomes very sensitive to any disorder and, to the author's knowledge, is never observed. However, this situation is worth studying here since the analytic solution available in this case offers a very clear picture of quasibifurcations, explaining their physical meaning.

To simplify matters it is convenient to rescale, $x \rightarrow x\lambda\mu_1^{1/2}, y \rightarrow y\lambda\mu_3^{1/2}$, i.e., to put $\lambda^2\mu_1 = 1, \lambda^2\mu_3 = 1$ in (1). The energy (1) can be equivalently represented as a sum over the real lattice:

$$F = Z \sum_{m,n} U(\mathbf{r}_{mn}), \quad \mathbf{r}_{mn} = ((m+an)a, nb). \quad (3)$$

In the limit $a, b \gg \lambda$, i.e., $|\mathbf{r}_{mn}| \gg 1$, the potential $U(r) = \int \exp(irk)(1+k^2)^{-1} d^2k$ becomes $\pi^{3/2} r^{-1/2} \times \exp(-r)$. Now, the key observation is that with exponential accuracy one can keep only the shortest vectors in the sum (3). However, a planar lattice can have only *one, two, or three* shortest vectors, so the infinite sum (3) is replaced by a sum of not more than three terms.

Moreover, the lattices with only one shortest vector cannot provide an energy minimum because of the following simple reason. By a small change of α one can always reach smaller F by making the shortest vector longer and keeping other vectors longer than the shortest one. Consequently, as candidates for minima one has to study only lattices with two or three equal shortest vectors, i.e., lattices having *rhombic unit cells*, edges of the rhombi being not longer than their diagonals. There is only one exception from this rule: the starting symmetric lattice having shortest vector \mathbf{r}_{10} .

Now, let us take a pair of lattice vectors $\mathbf{r}_{mn}, \mathbf{r}_{pq}$ and study when they form a rhombic unit cell. The first thing to notice is that the area of the unit cell has to be ab . Thus, we have $|mq - np| = 1$. Another constraint is that $|\mathbf{r}_{mn}| = |\mathbf{r}_{pq}|$. Simple algebra enables us to rewrite it as

$$(\alpha - \alpha_1)(\alpha - \alpha_2) + x^2 = 0, \quad \alpha_{1,2} = \frac{m \pm p}{n \pm q}, \quad (4)$$

where now $x = b/a$ [compare with (2)]. Equation (4) defines a circle in the (α, x) plane. However, we also have the constraint that the diagonals of the rhombus are not shorter than its edges: $|\mathbf{r}_{mn} \pm \mathbf{r}_{pq}| > |\mathbf{r}_{mn}|$. If written explicitly it defines an arc of the circle (4). But the conditions mentioned are not yet sufficient to provide an energy minimum. It turns out³ that one has to add the condition $(m+an)(p+aq) < 0$. The arcs selected by this complete set of constraints are shown in Fig. 4.

Let us observe that many arcs have common ends, thus forming continuous curves and reproducing the topology of Figs. 2 and 3 as well as quasibifurcations. Moreover, the system of arcs admits labeling. The generating numbers $m/n, p/q$ can be placed near ends of corresponding arcs so that labels of matching ends coincide. As demonstrated in Fig. 4 the labeling we get is exactly the Farey labeling introduced above.³

This result enables one to explain what happens when we go down in x along one arc and then change to another.

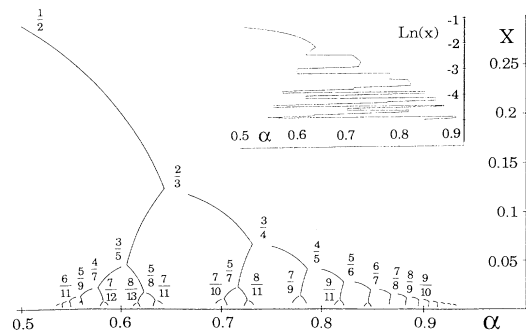


FIG. 4. Arcs of circles representing all rhombic lattices giving local minima of the energy (3) in the limit $a, b \gg \lambda$. After the ends of the circles are marked as explained in the text, Farey labeling is reproduced. Inset: Trajectory of the absolute energy minimum in the $(\alpha, \ln(x))$ plane.

er arc. While moving along the arc with the ends labeled by m/n and p/q , the shortest vectors of the lattice remain \mathbf{r}_{mn} and \mathbf{r}_{pq} . As x decreases the angle between \mathbf{r}_{mn} and \mathbf{r}_{pq} gets larger and reaches 120° at the end of the arc. At this point the lattice becomes triangular: $|\mathbf{r}_{mn} + \mathbf{r}_{pq}| = |\mathbf{r}_{mn}| = |\mathbf{r}_{pq}|$. After passing to the next arc the pair of shortest vectors changes: $\mathbf{r}_{mn}, \mathbf{r}_{pq} \rightarrow \mathbf{r}_{pq}, \mathbf{r}_{m+p, n+q}$ ($n < q$). The angle between the new shortest vectors is 60° ; it starts growing when x decreases further and it finally reaches 120° at the next end of the arc. Then the process is repeated. It should be noted that an alternative basis change, $\mathbf{r}_{mn}, \mathbf{r}_{pq} \rightarrow \mathbf{r}_{mn}, \mathbf{r}_{m+p, n+q}$ ($n < q$), leads to another arc which, however, is disconnected from the old arc. So, only one of two possible basis types is dynamically accessible from the end of the arc. The basis-replacement rule together with initial conditions immediately generates Fibonacci numbers (see Fig. 4).

We also can view this from another side. For any lattice one can choose two different bases: (i) $\mathbf{r}_{mn}, \mathbf{r}_{pq}$, being shortest lattice vectors, and (ii) $\mathbf{r}_{10}, \mathbf{r}_{01}$ defined by (3). In terms of the matrix \mathbf{A} transforming the first basis to the second one our result reads

$$\mathbf{A} = \begin{vmatrix} m & p \\ n & q \end{vmatrix} = \begin{vmatrix} F_{k-1} & F_k \\ F_k & F_{k+1} \end{vmatrix}, \quad (5)$$

for all dynamically accessible lattices. Geometrically this can be interpreted in the following way. Let us recognize \mathbf{r}_{10} as the horizontal period of the lattice. Now we connect every vortex with its four nearest neighbors and get two grids corresponding to the basis (i). Then we count how many times the horizontal period \mathbf{r}_{10} intersects each of the grids. According to (5) the count will give F_k and F_{k+1} .

Let us briefly characterize effects of disorder and temperature. Disorder becomes important at weak magnetic field when the density of vortices and, therefore, elastic moduli of the lattice are small. Thus large Fibonacci numbers are not likely to be reached. On the other hand, the effect of temperature is becoming unimportant in this limit: The danger is only thermal fluctuations destroying lattice topology through kink formation by dislocations, but the energy of a kink grows when the separation of vortices gets larger. However, thermal fluctuations must be important at high H and especially strong near the point of true bifurcation.⁸ Another thing to mention is that different regions of the lattice can leave the point $\alpha = \frac{1}{2}$ in different directions, creating domains of two types. However, computation of the energy of a domain wall gives a positive value,^{3,8} so one can hope that domains will be sufficiently large and thus observable.

Finally, let us mention that one can be interested also in the *absolute minimum* of the energy as function of x .

This question becomes relevant when the experiment lasts long enough to provide time for equilibration. The result for the case of exponential repulsion is shown in the inset of Fig. 4. The trace of the absolute minimum jumps from one branch of the tree to another in a complicated way leading to an infinite sequence of first-order transitions. One can notice that the curve passes through all common ends of pairs of arcs. The explanation is straightforward: These points correspond to perfect triangular lattices which are known to provide the absolute minimum of energy even without any constraint imposed by layers.

I thank A. Katz for drawing my attention to Ref. 2, and V. L. Pokrovskii for telling me about his findings^{6,8} before publication as well as for many helpful discussions. I also gratefully acknowledge important discussions with Alexander Sidorov in Moscow and with D. P. DiVincenzo at the University of Cornell where part of this work was done.

(a)Present address: Centre d'Etudes de Chimie Metallurgique, CNRS, 15, rue G. Urbain, F-94407 Vitry-sur-Seine CEDEX, France.

¹Phyllotaxis was discovered long ago and has its own interesting history. The following publications are sufficient for further references: D'Arcy W. Thompson, *On Growth and Form* (Cambridge Univ. Press, London, 1942), 2nd ed., Chap. 14; H. Weyl, *Symmetry* (Princeton Univ. Press, Princeton, 1952); N. Rivier, *Mod. Phys. Lett. B* **2**, 953 (1988).

²A.-J. Koch and F. Rothen, *J. Phys. (Paris)* **50**, 1603 (1989).

³L. S. Levitov (to be published).

⁴As possible real objects we mention novel Bi-based high- T_c materials where this kind of pinning was observed: A. Gupta, P. Esquinazi, H. F. Braun, and H.-W. Neumuller, *Phys. Rev. Lett.* **63**, 1869 (1989).

⁵For an artificial periodic structure providing pinning of vortices, see P. Martinoli, D. Daldini, C. Leemann, and E. Stoiker, *Solid State Commun.* **17**, 205 (1975).

⁶It turns out that the situation we are studying is stable with respect to small tilting of the magnetic field direction [V. L. Pokrovskii (private communication)].

⁷L. J. Campbell, M. M. Doria, and V. G. Kogan, *Phys. Rev. B* **38**, 2439-2443 (1988).

⁸B. I. Ivlev, N. B. Kopnin, and V. L. Pokrovskii, *J. Low Temp. Phys.* (to be published).

⁹Of course, it would be interesting to try to search for optimal vortex configurations in a wider class of solutions: nonprimitive periodic or, maybe, nonperiodic structures.

¹⁰V. G. Kogan, *Phys. Rev. B* **24**, 1572 (1981); A. V. Balatskii, L. I. Burlachkov, and L. P. Gor'kov, *Zh. Eksp. Teor. Fiz.* **90**, 1478 (1986) [*Sov. Phys. JETP* **63**, 866 (1986)]; L. I. Burlachkov, *Europhys. Lett.* **8**, 673 (1989).

¹¹G. H. Hardy and E. M. Wright, *An Introduction to the Theory of Numbers* (Clarendon, Oxford, 1954).